JCEC
THE JOURNAL OF ENGINEERING AND EXACT SCIENCES

OPEN ACCESS

The Journal of Engineering and Exact Sciences – jCEC, Vol. 08 N. 09 (2022)
journal homepage: https://periodicos.ufv.br/jcec
eISSN: 2527-1075
ISSN: 2446-9416

Hybrid Method for Predictive Transient Nonlinear Analysis of a Radiative-Convective Moving Porous Fin with Temperature-variant Internal Heat Generation

Article Info:
Article history: Received 2022-10-01/ Accepted 2022-11-14 / Available online 2022-11-15
doi: 10.18540/jcecvl8iss9pp14802-01i

CC BY

Gbeminiyi Musibau Sobamowo
ORCID: https://orcid.org/0000-0003-2402-1423
Department of Mechanical Engineering, Faculty of Engineering, University of Lagos, Akoka Lagos, Nigeria
E-mail: gsobamowo@unilag.edu.ng
Ridwan Oladotun Olagbadamosi
Department of Mechanical Engineering, Faculty of Engineering, Lagos State University, Epe Campus, Lagos, Nigeria
E-mail: olagbadamosiridwan@gmail.com
Arinola Bola Ajayi
ORCID: https://orcid.org/0000-0002-4733-0803
Department of Mechanical Engineering, Faculty of Engineering, University of Lagos, Akoka Lagos, Nigeria
E-mail: abajayi@unilag.edu.ng
Nehemiah Sabinus Alozie
ORCID: https://orcid.org/0000-0002-3840-3804
Department of Mechanical Engineering, Faculty of Engineering, University of Lagos, Akoka Lagos, Nigeria
E-mail: salozie@unilag.edu.ng
Antonio Marcos de Oliveira Siqueira
ORCID: https://orcid.org/0000-0001-9334-0394
Federal University of Viçosa, Brazil
E-mail: antonio.siqueira@ufv.br

Abstract
In this work, Laplace transform-Legendre-wavelet collocation method is adopted for a semi-numerical analysis of predicting transient nonlinear behaviour of a radiative-convective fin with temperature-variant internal heat generation. The verification of the results of the hybrid method shown good agreements with the direct numerical and approximate analytical method s in previous works. Parametric analysis depicts the significance of the model parameters in a way that it is found that as the convective-conductive and radiative-conductive parameters increase, temperature distribution decreases in the extended surface. The thermal distribution is augmented in the passive device as thermal conductivity is amplified. At the different positions in the fin, the temperature is enhanced as time progress. The semi-numerical solution provides a very good platform for the predictive analyses of the extended surfaces.
Keywords: Convective-radiative fin. Moving fin. Semi-numerical solution. Laplace transform-Legendre Wavelet Collocation method.

1. Introduction
Fins are used for augmentations of heat transfer rate in thermal and electronic components. Such important passive method of heat transfer enhancements has provoked several studies over the past decades [1-59]. The study of thermal behavior of continuous moving surfaces such as extrusion,

hot rolling, glass sheet or wire drawing, casting, powder metallurgy techniques for the fabrication of rod and sheet have become an area of increasing research interests. In the processes such as rolling of strip, hot rolling, glass fiber drawing, casting, extrusion, drawing of sheets and wires, there is usually the presence of heat exchange between surrounding and the stationary or moving material as depicted in Fig. 1 where hot plate/billet emerges from a die or furnace.

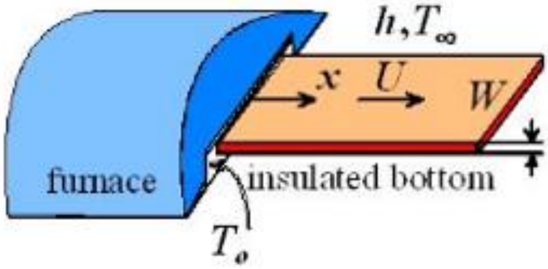

Fig. 1 Schematic diagram of rolling and extrusion

Since the schematic depicted in Figure 1 satisfies the approximate working condition of a heat exchanging device, they can be modeled as fins moving uninterruptedly. Due to these adaptable and wide areas of applications, there have been extensive research works on the continuous moving fins. Moreover, in industrial processes, control of cooling rate of the sheets is very important to obtain desired material structure. As a result, Torabi *et al.* [1], Aziz and Lopez [2], Aziz and Khani [3], Singh *et al.* [4], Aziz and Torabi [5], Ma *et al.* [6]. Sun [7], Kanth and Kumar [8] and the other authors [8-66] explored the thermal behaviour of a radiative-convective moving fins with temperature-variant thermal properties. These authors adopted various mathematical techniques to analyze the thermal problems [1-66].

The obvious non-power series semi-numerical solutions to the nonlinear problems are very much important. Such solutions allow effective thermal predictions of the extended surface over a large domain and time. Also, the semi-numerical solutions reduce the complex mathematical analysis that gives analytic expressions involving large number terms, high computational cost and time. Therefore, there is a need for comparatively flexible, simple, generic and highly accurate solutions. Legendre wavelet collocation is an easy and simple mathematical method with fast rate of convergence. To the best of the authors' knowledge, such application of the hybrid semi-numerical method for the heat transfer model of a moving convective-radiative porous fin under temperature-reliant internal heat generation has not been presented in literature. Such solutions provide effective predictions to extended surfaces' thermal performances. Therefore, in this study, Laplace transform-Legendre-wavelet collocation method is used to develop semi-numerical solutions for the nonlinear thermals of a moving convective-radiative porous fin under temperature-variant thermal conductivity.

2. Model Development for the Transient Thermal Flow Process

Fig. 2 presents an internally heated longitudinal porous moving fin of length L, thickness δ and perfectly and thermally attached to a prime surface at temperature T_b. Assuming that the porous fin tip is considered under adiabatic condition and the porous medium with fin material is homogeneous and isotropic for the unidirectional heat flow along the fin length. Also, local thermodynamic equilibrium prevails between the porous medium and the saturated with a single-phase fluid. The thermo-physical properties of the fin material and the fluid are constant, and the fluid density variation follows Boussinesq approximation.

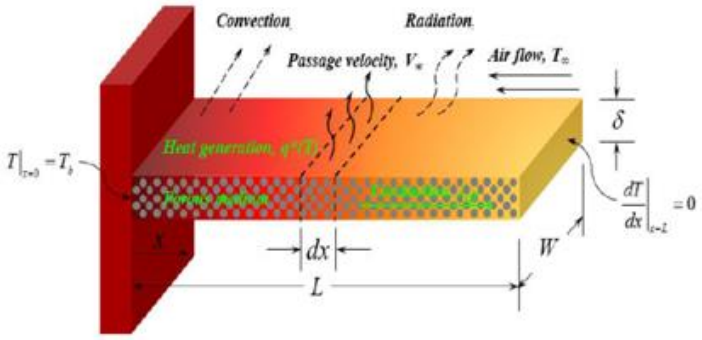

Fig. 2 Schematic of a longitudinal moving porous fin with perfect thermal contact and insulated tip

Using the assumptions stated above, the thermal energy balance equation (Fig. 3) of the extended surface is given by the following equation

Energy in left face + heat generated in element = energy out right face +energy lost by convection + energy lost by immersed fluid + energy lost by radiation + energy lost by moving +accumulated heat

(1)

$$q_x + q'''(T)A_{cr}dx = \left(q_x + \frac{\delta q}{\delta x}dx\right) + h(T)A_{suf}(T-T_a)(1-\phi) + \dot{m}c_p(T-T_a)$$
$$+\sigma\varepsilon(T)A_{suf}(T^4-T_s^4) + (\rho c_p)_{eff}A_{cr}u\frac{\partial T}{\partial x}dx + (\rho c_p)_{eff}A_{cr}\frac{\partial T}{\partial t}dx \quad (2)$$

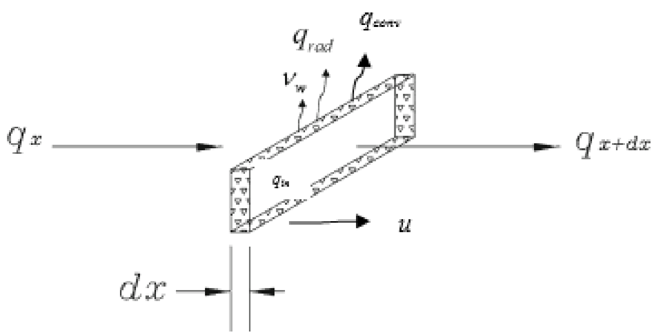

Fig. 3 Thermal energy balance in the elemental strip

Eq. (2) can be written as

$$q_x + (1-\phi)q'''(T)A_{cr}dx = \left(q_x + \frac{\delta q}{\delta x}dx\right) + hP(T-T_a)(1-\phi)dx + \dot{m}c_p(T-T_a)$$
$$+\sigma\varepsilon P(T^4-T_s^4)dx + (\rho c_p)_{eff}A_{cr}u\frac{\partial T}{\partial x} + (\rho c_p)_{eff}A_{cr}\frac{\partial T}{\partial t}dx \quad (3)$$

The rate of flow of fluid through the porous medium is given by

$$\dot{m} = \phi\rho_f V_w W dx \quad (4)$$

While the fluid flow velocity is and

$$V_w = \frac{gK\beta}{v}\left(T - T_a\right) \tag{5}$$

Therefore, after the substitution of Eq. (5) into Eq. (4), the mass flow rate of the fluid is given as

$$\dot{m} = \frac{\rho_f gK\beta W\phi}{v}\left(T - T_a\right)dx \tag{6}$$

The introduction of Eq. (7) into Eq. (3) produces Eq. (7)

$$\begin{aligned} &-\frac{\partial q}{\partial x} + \left(1-\phi\right)q'''\left(T\right)A_{cr}dx = hP\left(1-\phi\right)(T-T_a)dx + \frac{\rho_f c_{p,f} gK\beta W\phi(T-T_a)^2}{v}dx \\ &+\sigma\varepsilon P(T^4 - T_s^4)dx + \left(\rho c_p\right)_{eff} A_{cr}u\frac{\partial T}{\partial x} + \left(\rho c_p\right)_{eff} A_{cr}\frac{\partial T}{\partial t}dx \end{aligned} \tag{7}$$

Dividing Eq. (7) through by $A_{cr}dx$

$$\begin{aligned} &-\frac{1}{A_{cr}}\frac{\partial q}{\partial x} + \left(1-\phi\right)q'''\left(T\right) = \frac{hP\left(1-\phi\right)(T-T_a)}{A_{cr}} + \frac{\rho_f c_{p,f} gK\beta W\phi(T-T_a)^2}{vA_{cr}} \\ &+\frac{\sigma\varepsilon P(T^4 - T_s^4)}{A_{cr}} + \left(\rho c_p\right)_{eff} u\frac{\partial T}{\partial x} + \left(\rho c_p\right)_{eff}\frac{\partial T}{\partial t} \end{aligned} \tag{8}$$

Eq. (8) can be written as

$$\begin{aligned} &-\frac{1}{A_{cr}}\frac{\partial q}{\partial x} + \left(1-\phi\right)q'''\left(T\right) = \frac{hP\left(1-\phi\right)(T-T_a)}{A_{cr}} + \frac{\rho_f c_{p,f} gK\beta\phi(T-T_a)^2}{v\delta} \\ &+\frac{\sigma\varepsilon P(T^4 - T_s^4)}{A_{cr}} + \left(\rho c_p\right)_{eff} u\frac{\partial T}{\partial x} + \left(\rho c_p\right)_{eff}\frac{\partial T}{\partial t} \end{aligned} \tag{9}$$

The heat conduction rate through the solid portion of the fin is given by Fourier's law as given

$$q_s = -k_{eff}A_{cr}\frac{\partial T}{\partial x} \tag{10}$$

The radiation heat transfer rate in the porous medium is given as

$$q_p = -\frac{4\sigma A_{cr}\phi}{3\beta_R}\frac{\partial T^4}{\partial x} \tag{11}$$

Therefore, the total rate of heat transfer is given by

$$q = -k_{eff}A_{cr}\frac{\partial T}{\partial x} - \frac{4\sigma A_{cr}\phi}{3\beta_R}\frac{\partial T^4}{\partial x} \tag{12}$$

The introduction of Eq. (12) into Eq. (9) provides,

$$\frac{\partial}{\partial x}\left(k_{eff}\frac{\partial T}{\partial x}+\frac{4\sigma\phi}{3\beta_R}\frac{\partial T^4}{\partial x}\right)+\left(1-\phi\right)\dot{q}'''\left(T\right)=\frac{\rho_f c_{p,f} gK\beta\phi(T-T_a)^2}{v\delta}$$
$$+\frac{hP\left(1-\phi\right)(T-T_\infty)}{A_{cr}}+\frac{\sigma\varepsilon P(T^4-T_s^4)}{A_{cr}}+\left(\rho c_p\right)_{eff}u\frac{\partial T}{\partial x}+\left(\rho c_p\right)_{eff}\frac{\partial T}{\partial t} \tag{13}$$

Further simplification of Eq. (13) the governing differential equation for the fin becomes

$$\frac{\partial}{\partial x}\left(k_{eff}\frac{\partial T}{\partial x}\right)+\frac{4\sigma\phi}{3\beta_R}\frac{\partial}{\partial x}\left(\frac{\partial T^4}{\partial x}\right)-\frac{\rho_f c_{p,f} gK\beta\phi(T-T_a)^2}{v\delta}-\frac{hP\left(1-\phi\right)}{A_{cr}}(T-T_a)$$
$$-\frac{\sigma\varepsilon P}{A_{cr}}(T^4-T_s^4)+\left(1-\phi\right)q'''\left(T\right)=\left(\rho c_p\right)_{eff}u\frac{\partial T}{\partial x}+\left(\rho c_p\right)_{eff}\frac{\partial T}{\partial t} \tag{14}$$

The temperature-dependent thermal conductivity and internal heat generation are respectively given by the linear expressions as

$$k_{eff}=\left(1-\phi\right)k_s+\phi k_f \tag{15}$$

where,

$$q'''\left(T\right)=q_o'''\left[1+\gamma(T-T_a)\right] \tag{16}$$

And

$$\left(\rho c_p\right)_{eff}=\left(1-\phi\right)\left(\rho c_p\right)_s+\phi\left(\rho c_p\right)_f \tag{17}$$

Therefore, the governing equation becomes

$$k_{eff}\frac{\partial^2 T}{\partial x^2}+\frac{4\sigma\phi}{3\beta_R}\frac{\partial}{\partial x}\left(\frac{\partial T^4}{\partial x}\right)-\frac{\rho_f c_{p,f} gK\beta\phi(T-T_a)^2}{v\delta}-\frac{h_bP\left(1-\phi\right)\left(T-T_a\right)}{A_{cr}}$$
$$-\frac{\sigma\varepsilon_b P}{A_{cr}}\left(T^4-T_s^4\right)+\left(1-\phi\right)q_o'''\left[1+\gamma(T-T_a)\right]=\left(\rho c_p\right)_{eff}\left[u\frac{\partial T}{\partial x}+\frac{\partial T}{\partial t}\right] \tag{18}$$

For the case when the temperature between the base and tip of the fin is small, the radiative term can be linearized. Using Roseland's approximation for the radiative term in the model, with the aid of Taylor series, expanding T^4 about T_a

$$T^4\cong T_a^4+4T_a^3\left(T-T_a\right)+6T_a^2\left(T-T_a\right)^2+4T_a\left(T-T_a\right)^3+\ldots \tag{19}$$

and ignoring the higher order components in Eq. (21a), we have

$$T^4\cong 4T_a^3T-3T_a^4 \tag{20}$$

Therefore,

$$T^4-T_a^4\cong 4T_a^3\left(T-T_a\right) \tag{21}$$

Substituting Eq. (21) into the second term in the Eq. (18), we have

$$-\frac{4\sigma\phi}{3\beta_R}\frac{\partial T^4}{\partial x} = -\frac{4\sigma\phi}{3\beta_R}\frac{\partial(4T_a^3T - 3T_a^3)}{\partial x} = -\frac{16\sigma\phi T_a^3}{3\beta_R}\frac{\partial T}{\partial x} \tag{22}$$

Substituting Eqs. (21) and (22) into Eq. (18), we have

$$\begin{aligned} &k_{eff}\frac{\partial^2 T}{\partial x^2} + \frac{16\sigma\phi T_a^3}{3\beta_R}\frac{\partial^2 T}{\partial x^2} - \frac{\rho_f c_{p,f} gK\beta W\phi(T-T_a)^2}{vA_{cr}} - \frac{hP(1-\phi)}{A_{cr}}(T-T_a) \\ &-\frac{4\sigma\varepsilon PT_a^3}{A_{cr}}(T-T_a) + (1-\phi)q_o'''[1+\gamma(T-T_a)] = (\rho c_p)_{eff}\, u\frac{\partial T}{\partial x} + (\rho c_p)_{eff}\frac{\partial T}{\partial t} \end{aligned} \tag{23}$$

The initial condition is

$$T = T_0, \quad \text{when} \quad t = 0, \quad \text{for} \quad 0 < x < L, \tag{24}$$

The boundary conditions for the fin with insulated tip are given as

$$T = T_b, \quad \text{at} \quad x = 0, \text{for} \quad t > 0, \tag{25a}$$

$$\frac{dT}{dx} = 0, \quad \text{at} \quad x = L, \text{for} \quad t > 0, \tag{25b}$$

Eq. (23) can be expressed as

$$\begin{aligned} &\left(k_{eff} + \frac{16\sigma\phi T_a^3}{3\beta_R}\right)\frac{\partial^2 T}{\partial x^2} - \frac{\rho_f c_{p,f} gK\beta W\phi(T-T_a)^2}{vA_{cr}} - \frac{hP(1-\phi)}{A_{cr}}(T-T_a) \\ &-\frac{4\sigma\varepsilon PT_a^3}{A_{cr}}(T-T_a) + (1-\phi)q_o'''[1+\gamma(T-T_a)] = (\rho c_p)_{eff}\, u_o\frac{\partial T}{\partial x} + (\rho c_p)_{eff}\frac{\partial T}{\partial t} \end{aligned} \tag{26}$$

The temperature-dependent internal heat generation in the porous fin can be expressed as

$$q'''(T) = (1-\phi)q_o''' + (1-\phi)q_o'''\gamma T - (1-\phi)q_o'''\gamma T_a \tag{27}$$

Therefore

$$\begin{aligned} &\left(k_{eff} + \frac{16\sigma\phi T_a^3}{3\beta_R}\right)\frac{\partial^2 T}{\partial x^2} - \frac{\rho_f c_{p,f} gK\beta W\phi(T-T_a)^2}{vA_{cr}} - \frac{hP(1-\phi)}{A_{cr}}(T-T_a) - \frac{4\sigma\varepsilon PT_a^3}{A_{cr}}(T-T_a) \\ &+(1-\phi)q_o'''[1+\gamma(T-T_a)] = (\rho c_p)_{eff}\, u\frac{\partial T}{\partial x} + (\rho c_p)_{eff}\frac{\partial T}{\partial t} \end{aligned} \tag{28}$$

Collecting like terms, we have

$$\left(k_{eff}+\frac{16\sigma\phi T_a^3}{3\beta_R}\right)\frac{\partial^2 T}{\partial x^2}-\frac{\rho_f c_{p,f} gK\beta W\phi(T-T_a)^2}{vA_{cr}}-\left[\begin{matrix}\frac{hP(1-\phi)}{A_{cr}}+\frac{4\sigma\varepsilon PT_a^3}{A_{cr}}\\ -\left(\gamma(1-\phi)q_o'''\right)\end{matrix}\right](T-T_a)$$
$$+(1-\phi)q_o'''=\left(\rho c_p\right)_{eff}u\frac{\partial T}{\partial x}+\left(\rho c_p\right)_{eff}\frac{\partial T}{\partial t} \tag{29}$$

Which can be written as

$$\left(1+\frac{16\sigma\phi T_a^3}{3\beta_R k_{eff}}\right)\frac{\partial^2 T}{\partial x^2}-\frac{\rho_f c_{p,f} gK\beta W\phi(T-T_a)^2}{vA_{cr}k_{eff}}-\left[\begin{matrix}\frac{hP(1-\phi)}{A_{cr}k_{eff}}+\frac{4\sigma\varepsilon PT_a^3}{A_{cr}k_{eff}}\\ -\frac{\left(\gamma(1-\phi)q_o'''\right)}{k_{eff}}\end{matrix}\right](T-T_a)$$
$$+\frac{(1-\phi)q_o'''}{k_{eff}}=\frac{\left(\rho c_p\right)_{eff}u}{k_{eff}}\frac{\partial T}{\partial x}+\frac{\left(\rho c_p\right)_{eff}}{k_{eff}}\frac{\partial T}{\partial t} \tag{30}$$

Applying the following dimensionless variables

$$X=\frac{x}{L},\quad \theta=\frac{T-T_a}{T_b-T_a},\quad \tau=\frac{k_{eff}t}{\left(\rho c_p\right)_{eff}L^2} \tag{31}$$

Which implies that

$$x=XL,\quad T=\theta\left(T_b-T_a\right)+T_a,\quad T-T_a=\theta\left(T_b-T_a\right),\quad t=\frac{\tau\left(\rho c_p\right)_{eff}L^2}{k_{eff}} \tag{32}$$

When Eq. (32) is substituted into Eq. (30), we have

$$\left(1+\frac{16\sigma\phi T_a^3}{3\beta_R k_{eff}}\right)\frac{\partial^2\left[\theta\left(T_b-T_a\right)+T_a\right]}{\partial(XL)^2}-\frac{\rho_f c_{p,f} gK\beta W\phi\left[\theta\left(T_b-T_a\right)\right]^2}{vA_{cr}k_{eff}}$$
$$-\left[\begin{matrix}\frac{hP(1-\phi)}{A_{cr}k_{eff}}+\frac{4\sigma\varepsilon PT_a^3}{A_{cr}k_{eff}}\\ -\frac{\left(\gamma(1-\phi)q_o'''\right)}{k_{eff}}\end{matrix}\right]\theta\left(T_b-T_a\right)+\frac{(1-\phi)q_o'''}{k_{eff}} \tag{33}$$
$$=\frac{\left(\rho c_p\right)_{eff}u}{k_{eff}}\frac{\partial\left[\theta\left(T_b-T_a\right)+T_a\right]}{\partial(XL)}+\frac{\left(\rho c_p\right)_{eff}}{k_{eff}}\frac{\partial\left[\theta\left(T_b-T_a\right)+T_a\right]}{\partial\left(\frac{\left(\rho c_p\right)_{eff}L^2\tau}{k_{eff}}\right)}$$

Further simplification provides,

$$\left(1+\frac{16\sigma\phi T_a^3}{3\beta_R k_{eff}}\right)\frac{\left(T_b-T_a\right)}{L^2}\frac{\partial^2\theta}{\partial X^2}-\left(T_b-T_a\right)^2\frac{\rho_f c_{p,f} gK\beta W\phi\theta^2}{vA_{cr}k_{eff}}$$
$$-\left(T_b-T_a\right)\left[\frac{hP\left(1-\phi\right)}{A_{cr}k_{eff}}+\frac{4\sigma\varepsilon PT_a^3}{A_{cr}k_{eff}}-\frac{\left(\gamma\left(1-\phi\right)q_o'''\right)}{k_{eff}}\right]\theta \tag{34}$$
$$+\frac{\left(1-\phi\right)q_o'''}{k_{eff}}=\frac{\left(T_b-T_a\right)}{L}\frac{\left(\rho c_p\right)_{eff}u}{k_{eff}}\frac{\partial\theta}{\partial X}+\frac{\left(T_b-T_a\right)}{L^2}\frac{\partial\theta}{\partial\tau}$$

Which gives

$$\left(1+\frac{16\sigma\phi T_a^3}{3\beta_R k_{eff}}\right)\frac{\partial^2\theta}{\partial X^2}-\frac{\rho_f c_{p,f} gK\beta W\phi L^2\left(T_b-T_a\right)\theta^2}{vA_{cr}k_{eff}}$$
$$-\left[\frac{hP\left(1-\phi\right)L^2}{A_{cr}k_{eff}}+\frac{4\sigma\varepsilon PT_a^3L^2}{A_{cr}k_{eff}}-\frac{\left(\gamma\left(1-\phi\right)q_o'''\right)L^2}{k_{eff}}\right]\theta \tag{35}$$
$$+\frac{\left(\left(1-\phi\right)q_o'''\right)L^2}{k_{eff}\left(T_b-T_a\right)}=\frac{\left(\rho c_p\right)_{eff}uL}{k_{eff}}\frac{\partial\theta}{\partial X}+\frac{\partial\theta}{\partial\tau}$$

The above equation can be written as

$$\left(1+4R\right)\frac{\partial^2\theta}{\partial X^2}-S_h\theta^2-\left(Mc+Mr-Q_{\gamma e}\right)\theta+Q_e=Pe_e\frac{\partial\theta}{\partial X}+\frac{\partial\theta}{\partial\tau} \tag{36}$$

where

$$Rd=\frac{16\sigma\phi T_a^3}{3\beta_R k_{eff}},\quad Mc^2=\frac{hP\left(1-\phi\right)L^2}{A_{cr}k_{eff}},\quad Mr=\frac{4\sigma\varepsilon PT_a^3L^2}{A_{cr}k_{eff}},Q=\frac{\left(1-\phi\right)q_o'''L^2}{k_{eff}\left(T_b-T_a\right)},$$
$$Pe=\frac{\left(\rho c_p\right)_{eff}u_oL}{k_{eff}},\quad S_h=\frac{\rho_f c_{p,f} gK\beta W\phi L^2\left(T_b-T_a\right)}{vA_{cr}k_{eff}} \tag{37}$$

Eq. (36) is alternative written as

$$\frac{\partial^2\theta}{\partial X^2}-S_p\theta^2-\left(Mc+Nr-\gamma Q\right)\theta+Q=Pe_R\frac{\partial\theta}{\partial X}+\zeta\frac{\partial\theta}{\partial\tau} \tag{38}$$

where

$$Nc=\frac{Mc}{1+4R},\quad Nr=\frac{Mr}{1+4R}\quad S_p=\frac{S_h}{1+4R},\quad Q_\gamma=\frac{Q_{\gamma e}}{1+4R},$$
$$Q=\frac{Q_e}{\left(1+4R\right)},\quad Pe_R=\frac{Pe_e}{\left(1+4R\right)},\quad \zeta=\frac{1}{\left(1+4R\right)} \tag{39}$$

Also, the nondimensionalization for the initial and boundary conditions can be done by substituting Eq. (32) into Eqs. (24) and (25)

The initial condition is

$$\theta\left(T_b - T_a\right) + T_a = T_0 \quad \text{when} \quad \frac{\tau\left(\rho c_p\right)_{eff} L^2}{k_{eff}} = 0, \quad \text{for} \quad 0 < XL < L, \tag{40}$$

The boundary conditions for the fin with insulated tip are given as

$$\theta\left(T_b - T_a\right) + T_a = T_b, \quad \text{at} \quad XL = 0 \quad \text{for} \quad \frac{\tau\left(\rho c_p\right)_{eff} L^2}{k_{eff}} > 0, \tag{41a}$$

$$\frac{\partial\left[\theta\left(T_b - T_a\right) + T_a\right]}{\partial(XL)} = 0, \quad \text{at} \quad XL = L, \text{for} \quad \frac{\tau\left(\rho c_p\right)_{eff} L^2}{k_{eff}} > 0, \tag{41b}$$

Therefore, the adimensional initial condition is

$$\theta = \theta_0 \quad \text{when} \quad \tau = 0, \quad \text{for} \quad 0 < X < 1, \tag{42}$$

Also, the dimensionless boundary conditions are given as

$$\theta = 1, \quad \text{at} \quad X = 0 \quad \text{for} \quad \tau > 0, \tag{43a}$$

$$\frac{\partial \theta}{\partial X} = 0, \quad \text{at} \quad X = 1, \text{for} \quad \tau > 0, \tag{43b}$$

3. Method of Solution: Laplace transform-Legendre Wavelet Collocation Method

The developed nonlinear in Eq. (38) alongside with the initial and boundary conditions are solved using the hybrid method. The procedures of the applications are stated as follows:

3.1. Laplace transform method (LT)

The LT of function *f(t)* and corresponding inversion are enumerated as

$$\Theta(s) = \int_0^{\infty} e^{-st}\theta(\tau)d\tau \tag{44}$$

$$\theta(\tau) = \frac{1}{2\pi i}\int_{s-i\infty}^{s+i\infty} e^{-s\tau}\Theta(s)d\tau \tag{45}$$

where $s=a+ib$ $(a, b \in R)$ is a complex number.

3.2 Applying Laplace Transform method to the Nonlinear Thermal Model

Applying Laplace transform to Eq. (38), provides the following solutions

$$\frac{d^2\tilde{\theta}}{dX^2} - S_h\tilde{\theta}^2 - Mc\tilde{\theta} - Nr\tilde{\theta} + \frac{Q}{s} + Q\gamma\tilde{\theta} = \zeta s\tilde{\theta} + Pe_R\frac{\partial\tilde{\theta}}{\partial X} \tag{46}$$

Collecting like terms, we have

$$\frac{d^2\tilde{\theta}}{dX^2} - Pe_R\frac{d\tilde{\theta}}{dX} - S_h\tilde{\theta}^2 - \left(\zeta s + Mc + Nr + Q\gamma\right)\tilde{\theta} + \frac{Q}{s} = 0 \tag{47}$$

with boundary conditions in Laplace domain are

$$\begin{aligned} &s > 0, \quad X = 0, \quad \frac{\partial\tilde{\theta}}{\partial x} = 0 \\ &s > 0, \quad X = 1, \quad \tilde{\theta} = \frac{1}{s} \end{aligned} \tag{48}$$

3.3 The Principle and Procedure of Legendre Wavelet Collocation Method

Eq. (47) is still nonlinear after finding the Laplace transform of the governing equation, in order to solve the nonlinear equation, Legendre wavelet collocation method is applied. The principle and the procedure of the method is described as given below.

Wavelets: The formula for the continuous wavelet are defined as

$$\tilde{\psi}_{a,b}\left(X\right) = \left|a\right|^{\frac{-1}{2}}\tilde{\psi}\left(\frac{X-b}{a}\right), a, b \in R, a \neq 0 \tag{49}$$

The dilation and translation parameters are given as *a* and *b*, respectively.

The Legendre wavelets defined on the interval [0, 1] is given by

$$\tilde{\psi}_{n,m}\left(X\right) = \begin{cases} \sqrt{\left(m+\frac{1}{2}\right)}2^{k/2}\tilde{P}_m\left(2^kX-\hat{n}\right), & \frac{\hat{n}-1}{2^k} \leq \frac{\hat{n}-1}{2^k} \\ 0 & otherwise \end{cases} \tag{50}$$

where m=0,1,…,M-1 and n=1,2,...2^{k-1}. $\tilde{P}_m\left(X\right)$ *is the Legendre polynomial of order m in Laplace domain.*

$$\tilde{P}_0\left(X\right) = \frac{1}{s}, \tilde{P}_1\left(X\right) = \frac{X}{s},$$

$$\tilde{P}_{m+1}\left(X\right) = \frac{2m+1}{m+1}X\tilde{P}_m\left(X\right) - \frac{m}{m+1}\tilde{P}_{m-1}\left(X\right), \tag{51}$$

$m = 1, 2, 3......, M-1.$

A function $\tilde{f}\left(X\right)$ defined in domain [0, 1] can be expressed as

$$\tilde{f}(X) = \sum_{n=1}^{\infty}\sum_{m=0}^{\infty} c_{n,m}\tilde{\psi}_{n,m}(X) \tag{52}$$

where $c_{n,m} \leq \tilde{f}(X), \tilde{\psi}_{n,m}(X) >$ in which <…> denotes the inner product

Taking some terms in infinite series, then Eq. (52) can be written as

$$\tilde{f}(X) = \sum_{n=1}^{2^{k-1}}\sum_{m=0}^{M-1} c_{n,m}\tilde{\psi}_{n,m}(X) = C^T\tilde{\psi}(X) \tag{53}$$

Where C and $\tilde{\psi}(X)$ are M x1 matrices given by

$$C = \left[c_1, 0, c_1, 1, ..., c_1, M-1, c_2, 1, ..., c_2, M-1, c_{2^{k-1}}, 1, ..., c_{2^{k-1}}, M-1\right]^T \tag{54}$$

$$\tilde{\psi}(X) = \begin{bmatrix} \tilde{\psi}_{1},_{0}(X), \tilde{\psi}_{1,1}(X), ..., \tilde{\psi}_{1,M-1}(X), \tilde{\psi}_{2,0}(X), ..., \\ \tilde{\psi}_{2,M-1}(X), ..., \tilde{\psi}_{2^{k-1}},_{0}(X), \tilde{\psi}_{2^{k-1},1}(X), ..., \psi_{2^{k-1}},_{M-1}(X) \end{bmatrix}^T$$

(i) Property of the product of two Legendre wavelets

The following property can be written if E is a given wavelets vector,

$$E^T\tilde{\psi}\tilde{\psi}^T = \tilde{\psi}^T\hat{E} \tag{55}$$

(ii) Operational matrix of integration: From Eq. (52), the integration of wavelets $\tilde{\psi}(X)$ can be written as

$$\int_0^X \tilde{\psi}(s)ds = \tilde{P}\tilde{\psi}(X), X \in [0,1]$$

where P is $2^{k-1}M$ x *$2^{k-1}M$,* the operational matrix of integration is given by

$$P = \frac{1}{2}\begin{pmatrix} 1 & \frac{1}{3} & 0 & \cdots & \cdots & \cdots & \cdots & 0 \\ \frac{-1}{\sqrt{3}} & 0 & \frac{1}{\sqrt{15}} & \cdots & \cdots & \cdots & \cdots & 0 \\ 0 & \frac{-1}{\sqrt{15}} & 0 & \cdots & \cdots & \cdots & \cdots & 0 \\ \vdots & \vdots & \vdots & \ddots & & & & \vdots \\ \vdots & \vdots & \vdots & & \ddots & & & \vdots \\ \vdots & \vdots & \vdots & & & \ddots & & \vdots \\ 0 & 0 & 0 & \cdots & \cdots & \cdots & \ddots & \frac{\sqrt{2M-3}}{(2M-3)\sqrt{2M-1}} \\ 0 & 0 & 0 & \cdots & \cdots & \cdots & \cdots & \frac{-\sqrt{2M-3}}{(2M-3)\sqrt{2M-1}} \end{pmatrix} \tag{56}$$

3.4 Application of Legendre Wavelet Collocation Method to the Nonlinear Thermal Model

In order to apply the Legendre wavelet collocation method to the nonlinear thermal model, let

Let $\tilde{\theta}''(X) = C^T \tilde{\psi}(X)$ (57)

If we integrate Eq. (57) with respect to *X* from 0 to *X*, one obtains

$$\tilde{\theta}'(X) = \tilde{\theta}'(0) + C^T \tilde{P}\tilde{\psi}(x) \qquad \Rightarrow \tilde{\theta}'(X) = C^T \tilde{P}\tilde{\psi}(x) \quad since \quad \tilde{\theta}'(0) = 0 \tag{58}$$

Now, on integrating Eq. (58) and apply the boundary conditions, we get

$$\tilde{\theta}(X) = \tilde{\theta}(0) + C^T \tilde{P}^2 \tilde{\psi}(X) \tag{59}$$

If we Put *X=1* in Eq. (59), we have

$$\tilde{\theta}(0) = \frac{1}{s} - C^T \tilde{P}^2 \tilde{\psi}(1) \text{, since } \theta(1) = 1 \text{, we obtain} \tag{60}$$

If we substitute Eq. (60) into Eq. (58)

$$\tilde{\theta}'(X) = \frac{1}{s} - C^T \tilde{P}^2 \tilde{\psi}(1) + C^T \tilde{P}^2 \tilde{\psi}(X) \tag{61}$$

Again, the integrating of Eq. (61), with respect to *X* from *0* to *X*, one arrives at

$$\tilde{\theta}(X) = \frac{1}{s} - C^T \tilde{P}^2 \tilde{\psi}(1) d'\tilde{P}\tilde{\psi}(X) + C^T \tilde{P}^2 \tilde{\psi}(X) \tag{62}$$

The Substitution of $\tilde{\theta}''(X)$, $\tilde{\theta}'(X)$ and $\tilde{\theta}(X)$ in Eqs. (57), (61) and (62) into Eq. (47), produced

$$\begin{gathered} C^T \tilde{\psi}(X) - Pe_R\left(\frac{1}{s} - C^T \tilde{P}^2 \tilde{\psi}(1) + C^T \tilde{P}^2 \tilde{\psi}(X)\right) - S_h\left(\frac{1}{s} - C^T \tilde{P}^2 \tilde{\psi}(1) d'\tilde{P}\tilde{\psi}(X) + C^T \tilde{P}^2 \tilde{\psi}(X)\right)^2 \\ -(\zeta s + Mc + Nr + Q\gamma)\left(\frac{1}{s} - C^T \tilde{P}^2 \tilde{\psi}(1) d'\tilde{P}\tilde{\psi}(X) + C^T \tilde{P}^2 \tilde{\psi}(X)\right) + \frac{Q}{s} = R(X, c_1, c_2, \ldots, c_n) \end{gathered} \tag{63}$$

n collocation points is chosen i.e. X_i, $i = 1,2,3,\ldots,n$ in the interval (0,1), at which residual $R(X, c_i)$ equal to zero. It should be noted that the number of such points gives the number of coefficient c_i, $i = 1,2,3,\ldots,n$.

$$C = \left[c_1, 0, c_1, 1, \ldots, c_1, M-1, c_2, 1, \ldots, c_2, M-1, c_{2^{k-1}}, 1, \ldots, c_{2^{k-1}}, M-1\right]^T \tag{64}$$

Thus, we arrives at $R(X, c_1, c_2, c_3, \ldots, c_n) = 0$, $i = 1,2,3,\ldots,n$.

The above Eq. (63) gives a system of nonlinear equations which are solved simultaneously using Newton-Raphson method after the numerical inversion of the Laplace transform [67] and the values of C are obtained. When the values of C are substituted into Eq. (62), the solution of $\theta(X)$ is found.

4. Results and Discussion

The simulated results and parametric studies on the passive device are presented in this section. The effect of each parameter of the thermal model on the thermal behaviour of the extended surface is investigated. The results are presented in various sub-sections for better analysis and understanding. In Table 1, the results of the present study are compared with the results of the previous studies in literature using the following parameters $Nc=0.30$, $S_h=0.10$, $Q=0.40$ and $\gamma=0.20$.

Table 1: Comparison of results

X	NUM	LTLWCM	HPM [68]	VPM [69]
0.00	0.934213428	0.934213444	0.934213428	0.934213432
0.10	0.934856715	0.934856727	0.934856715	0.934856719
0.20	0.936788309	0.936788323	0.936788310	0.936788315
0.30	0.940013429	0.940013444	0.940013429	0.940013435
0.40	0.944540802	0.944540815	0.944540802	0.944540807
0.50	0.950382714	0.950382725	0.950382714	0.950382721
0.60	0.957555079	0.957555090	0.957555080	0.957555084
0.70	0.966077531	0.966077540	0.966077531	0.966077536
0.80	0.975973531	0.975973539	0.975973531	0.975973535
0.90	0.987270505	0.987270501	0.987270505	0.987270508
1.00	1.000000000	1.000000000	1.000000000	1.000000000

The influence of dimensionless time on moving porous fin thermal distribution is shown in Fig. 4. The temperature history increases with increasing time value. This is expected because with increasing heat transfer rate, the porous fin conducts more heat, thus temperature increases.

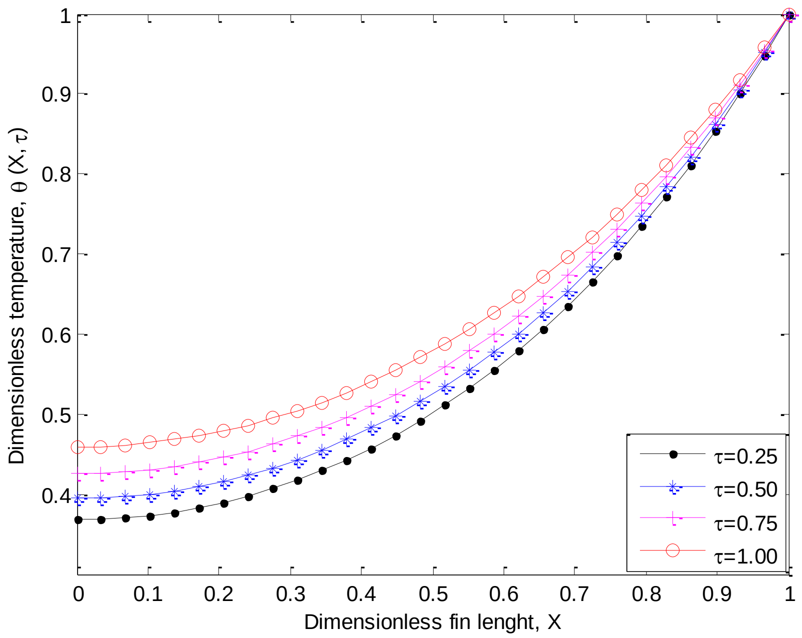

Fig. 4 Dimensionless temperature distribution at different time in the fin

Figures 5-8 displays the impacts of porous, convective-conductive, radiative-conductive and Peclet numbers on the thermal behaviour of the fin. It is shown in the figures that the porous, convective-conductive, radiative-conductive and Peclet numbers have significant effects on the heat transfer in the porous fin. The results depicted that as the porous, convective-conductive, radiative-conductive and Peclet numbers increase, the dimensionless temperature distribution in the fin decreases and consequently, the rate of heat transfer by the fin increases.

The swift reduction in temperature is because as these parameters increase, more heat is lost from the fin because the heat transfer rate is enhanced, and more cooling of the fin occurs which shows a decrease in the temperature profile and consequently, the fin thermal performance is increased. The effect of *Pe* on temperature distribution in the moving porous fin is shown in Fig. 8. An increase in *Pe* resulted in decreasing values of thermal distribution within the extended surface. This is expected because increasing *Pe* augments material motion and reduces exposure time to environment. Hence, fin temperature history intensifies.

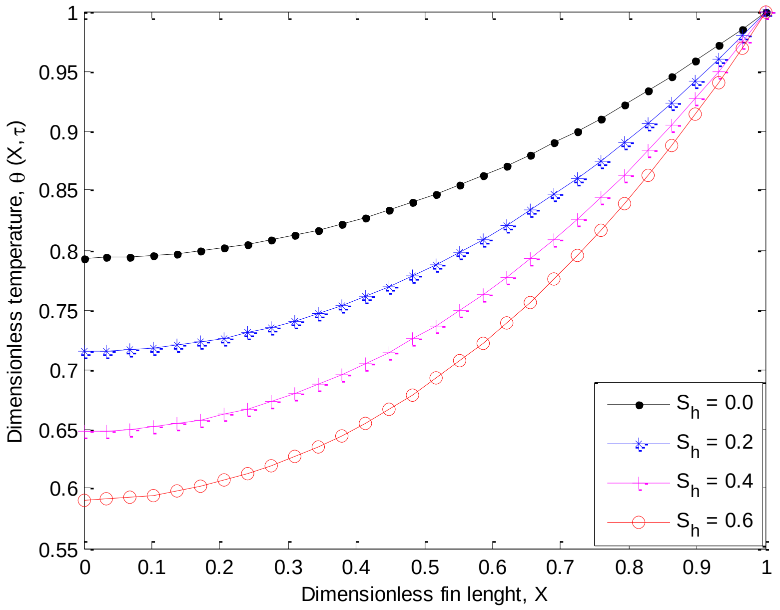

Fig. 5 Effect of porosity on the dimensionless temperature distribution in the fin

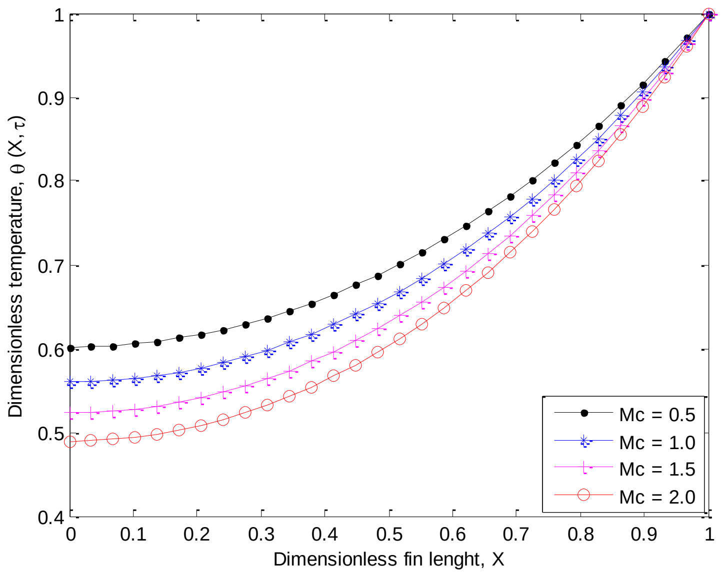

Fig. 6 Effect of convective-conductive number on the temperature distribution in the fin

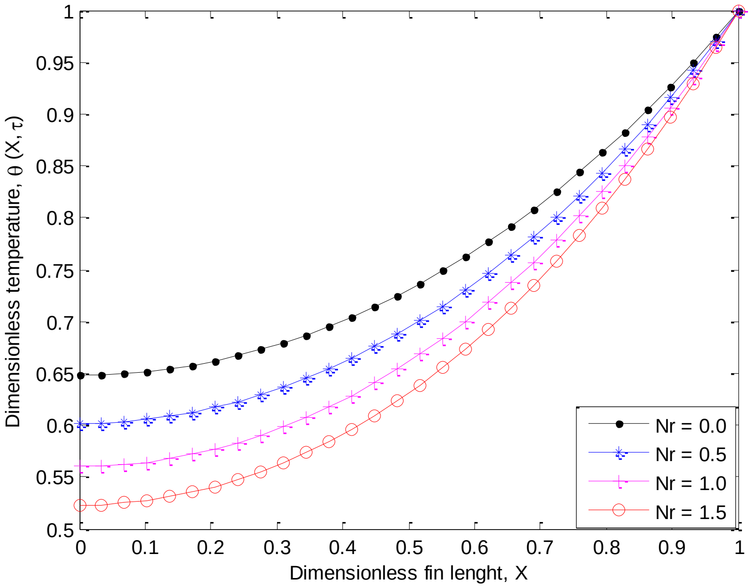

Fig. 7 Effect of radiative-conductive number on the temperature distribution in the fin

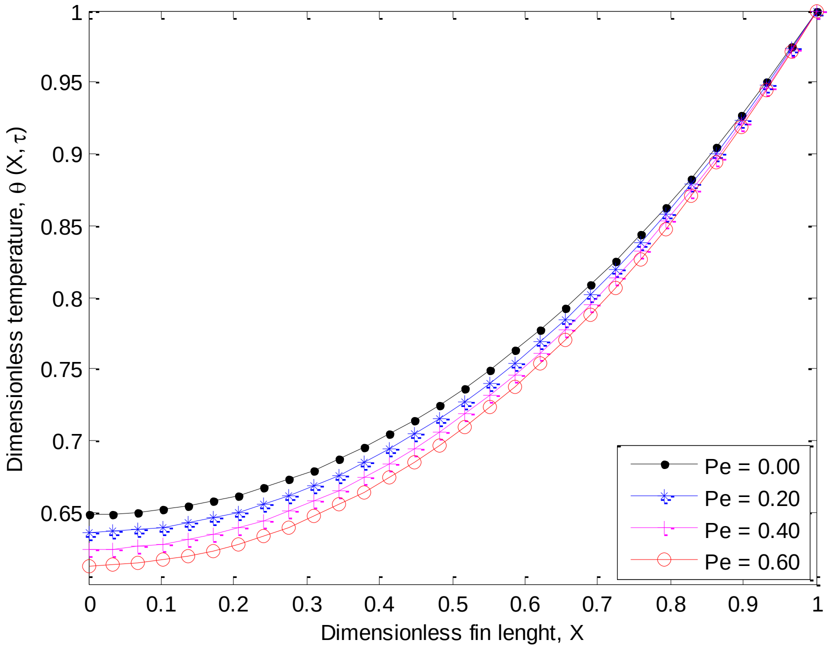

Fig. 8 Effect of convective-conductive number on the temperature distribution in the fin

The effect of internal heat generation on temperature distribution in the moving porous fin is shown in Fig. 9. An increase in internal heat generation resulted in increasing values of thermal distribution within the extended surface. This is expected because increasing *Pe* augments material motion and reduces exposure time to environment. Hence, fin temperature history intensifies.

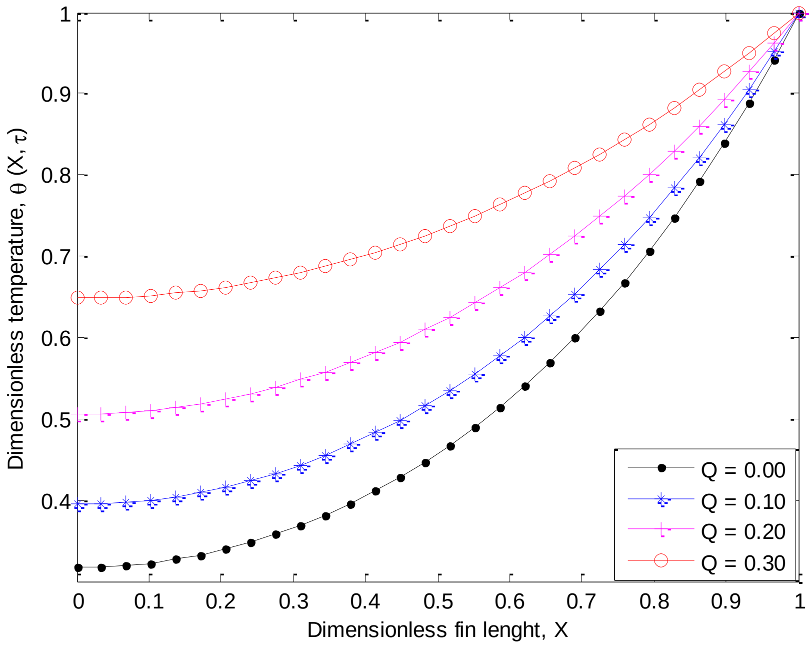

Fig. 9 Effect of internal heat generation on the temperature distribution in the fin

Fig. 10 shows the impacts of radiative number on the dimensionless temperature profiles along the fin length. It is shown in the figures that the radiative number, *Rd* has considerable impact on the fin thermal performance The results depicted that as the radiative number increases, the dimensionless temperature distribution in the fin also increases and consequently, the rate of heat transfer by the fin decreases.

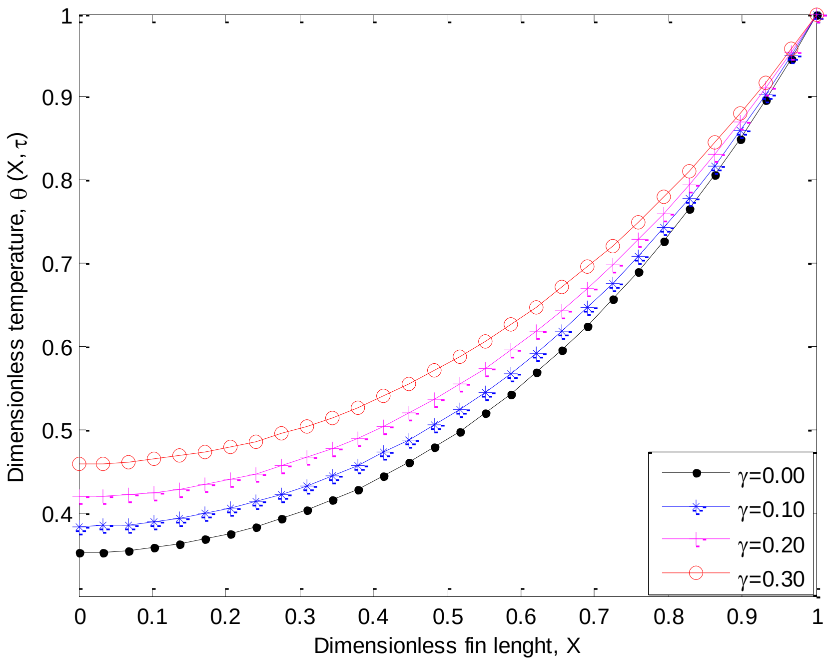

Fig. 10 Effect of temperature-dependent internal heat generation parameter on the temperature distribution in the fin

5. Conclusion

The present study developed a semi-numerical analysis of transient nonlinear thermal model of radiative-convective fin with varying internal heat generation using Laplace transform-Legendre-wavelet collocation method. Thereafter, parametric studies were carried out. The research outcomes establish that the temperature history increases with increasing time value. When the porous, convective-conductive and radiative-conductive parameters increase, the dimensionless temperature distribution in the fin decreases and consequently, the rate of heat transfer by the fin increases. An increase in *Pe* resulted in increasing values of thermal distribution within the extended surface. However, as the radiative number increases, the dimensionless temperature distribution in the fin also increases and consequently, the rate of heat transfer by the fin decreases. The semi-numerical solutions in the present work will serve as basis for comparisons for the numerical and approximate analytical solutions of the subsequent works on the thermal analysis of the extended surfaces. Moreover, the parametric studies established that the controlling parameters of the fin during operation should be prudently selected to make sure that it retains its principal function of heat removal from the main surface.

Nomenclature

A_{cr} fin cross sectional area, m^2
B_o magnetic field intensity, Tesla or kg/sec^2Amp
c_{pa} specific heat capacity, J/kgK
h coefficient of convective heat transfer, W/m^2K
J_c conduction current intensity, A
k fin thermal conductivity, W/mK
k_b fin thermal conductivity at the base temperature, W/mK
L fin length , M
Mc adimensional convective parameter
Nr adimensional radiation parameter
P fin perimeter, m
Pe Peclet number
t time, sec.
T fin temperature, K
T_∞ ambient temperature, K
T_b fin temperature at the base, K
x fin axial distance, m
X adimensional fin length

Greek Symbols

δ fin thickness , m
θ adimensional temperature
θ_b adimensional temperature at the fin base
ρ fin material density, kg/m^3
σ Stefan-Boltzmann constant, W/m^2K^4
σ Electrical conductivity, $\Omega^{-1}m^{-1}$ or sec^2Amp^2/kgm^3

References

[1] M. Torabi, H. Yaghoobi and A. Aziz Analytical Solution for Convective-Radiative Continuously Moving Fin with Temperature-Dependent Thermal Conductivity Int. J. Thermophysics (2012) 33: 924-941.

[2] A. Aziz and R. J. Lopez, Convection -radiation from a continuously moving, variable thermal conductivity sheet or rod undergoing thermal processing, I. J. of Thermal Sciences 50 (2011), 1523-1531.

[3] A. Aziz, F. Khani, Convection-radiation from a continuously moving fin of variable thermal conductivity, J. of Franklin Institute, 348 (2011), 640-651.

[4] S. Singh, D. Kumar,K. N. Rai. Wavelet Collocation Solution for Convective-Radiative Continuously Moving Fin with Temperature-Dependent Thermal Conductivity. International Journal of Engineering and Advanced Technology, 2(4), 2013.

[5] A. Aziz, M. Torabi, Covective-radiative fins with simultaneous variation of thermal conductivity, heat transfer coef ficient and surface emissivity with temperature, Heat transfer Asian Research 41 (2) (2012).

[6] J. Ma, Y. Sun, B. W. Li, H. Chen Spectral collocation method for radiative–conductive porous fin with temperature dependent properties. Energy Conversion and Management 111 (2016) 279–288.

[7] Y. Sun J. Ma, B. W. Li, H. Spectral collocation method for convective-radiative transfer of a moving rod with variable thermal conductivity. International Journal of Thermal Sciences 90 (2015) 187-196.

[8] A.S.V. R. Kanth and N. U. Kumar. Application of the Haar Wavelet Method on a Continuously Moving Convective-Radiative Fin with Variable Thermal Conductivity. Heat Transfer—Asian Research. DOI. 42(4)(2013), 1-17.

[9] A. S. V. R. Kanth and N. U. Kumar. A Haar Wavelet Study on Convective-Radiative Fin under Continuous Motion with Temperature-Dependent Thermal Conductivity. Walailak J Sci & Tech. 11(3)(2014), 211-224.

[10] R. K. Singla and D. Ranjan. Application of decomposition method and inverse parameters in a moving fin, Energy Conversion and Management, 84(2014), 268-281

[11] A. Moradi and R. Rafiee. Analytical Solution to Convection-Radiation of a Continuously Moving Fin with Temperature-Dependent thermal conductivity, Thermal Science, 17(2003), 1049-1060.

[12] A. S. Dogonchi and D. D. Ganji. Convection-Radiation heat transfer study of moving fin with temperature dependent thermal conductivity, heat transfer coefficient and heat generation, Applied Thermal Engineering, 103(2016), 705-712

[13] Y. S. Sun and J. Ma. Application of Collocation Spectral Method to Solve a Convective – Radiative Longitudinal Fin with Temperature Dependent Internal Heat Generation, Thermal Conductivity and Heat Transfer Coefficient, Journal of Computational and Theoretical Nano-science, volume12(2015), 2851- 2860.

[14] M. G. Sobamowo, A. A. Yinusa, M. O. Salami, O. C. Osih, B. O. Adesoye. Heat Transfer Analysis of a Rectangular Moving Porous Fin with Temperature-Dependent Thermal Conductivity and Internal Heat Generation: Comparative and Parametric Studies. Engineering Advances. 1(2)(2021), 50-66.

[15] T. Y. Kim, D. K. Kim, S. J. Kim. Scroll heat sink: A novel heat sink with the moving fins inserted between the cooling fins. International Journal of Heat and Mass Transfer 51(2008), 3267–3274.

[16] M.C. Jayaprakash, H. A.H. Alzahrani b, G. Sowmya, R.S. Varun Kumar, M. Y. Malik, A. Alsaiari, B.C. Prasannakumara. Thermal distribution through a moving longitudinal trapezoidal fin with variable temperature-dependent thermal properties using DTM-Pade approximant. Case Studies in Thermal Engineering 28 (2021) 101697.

[17] M. Turkyilmazoglu. Heat transfer from moving exponential fins exposed to heat generation. International Journal of Heat and Mass Transfer, 116(2018), 346-351.

[18] A. Moradi, R. Rafiee. Analytical Solution to Convection-Radiation of a Continuously Moving Fin with Temperature-Dependent Thermal Conductivity. Thermal Science. 17(4)(2013), 1049-1060
[19] A. Moradi, A. P. M. Fallah, T. Hayat, T., O. M. Aldossary. “On Solution of Natural Convection and Radiation Heat Transfer Problem in a Moving Porous Fin. Arabian Journal for Science and Engineering, 39(2014), 1303-1312.
[20] P. L. Ndlovu. Numerical analysis of transient heat transfer in radial porous moving fin with temperature dependent thermal properties Journal of Applied and Computational Mechanics 6 (1)(2020), 137-144
[21] P. L. Ndlovu. Analytical Study of Transient Heat Transfer in a Triangular Moving Porous Fin with Temperature Dependant Thermal Properties. Defect and Diffusion Forum. 393 (2019), 31–46.
[22] P. L. Ndlovu and R. J. Moitsheki. Thermal Analysis of Natural Convection and Radiation Heat Transfer in Moving Porous Fins. Frontiers in Heat and Mass Transfer (FHMT), 12(2019), 7-15.
[23] P. L. Ndlovu and R. J. Moitsheki. Steady state heat transfer analysis in a rectangular moving porous fin. Propulsion and Power Research. 2020(9), 188-196
[24] P. L. Ndlovu and R. J. Moitsheki.. Analysis of transient heat transfer in radial moving fins with temperature-dependent thermal properties. Journal of Thermal Analysis & Calorimetry. 138(4)(2019), 2913-2921.
[25] P. L. Ndlovu and R. J. Moitsheki. Analysis of temperature distribution in radial moving fins with temperature dependent thermal conductivity and heat transfer coefficient. International Journal of Thermal Sciences 145(2019), 106-115
[26] P. L. Ndlovu and R. J. Moitsheki. A Study of Transient Heat Transfer through a Moving Fin with Temperature Dependent Thermal Properties. Defect and Diffusion Forum 401(2020), 1-13.
[27] P. L. Ndlovu and R. J. Moitsheki. Analysis of a Convective-Radiative Continuously Moving Fin with Temperature-Dependent Thermal Conductivity. International Journal of Nonlinear Sciences and Numerical Simulation. 21(2020).
[28] G. Sowmya, B. J. Gireesha, M. Madhu, Macha 2020. "Analysis of a fully wetted moving fin with temperature-dependent internal heat generation using the finite element method" Heat transfer, 49(4)(2020): 1939-1954.
[29] B. J., Gireesha, G., Sowmya, S., Sindhu. Analysis of thermal behavior of moving longitudinal porous fin wetted with water-based SWCNTs and MWCNTs. Heat transfer, 49(4)(2020): 2044~2058
[30] G. Sowmya, Bijjanal Jayanna Gireesha, Analysis of heat transfer through different profiled longitudinal porous fin by differential transformation method, Heat Transfer, 10.1002/htj.22394, **51**, 2, (2165-2180), (2021).
[31] B.J. Gireesha, G. Sowmya, Madhu Macha. Temperature distribution analysis in a fully wet moving radial porous fin by finite element method", International Journal of Numerical Methods for Heat & Fluid Flow. 2019.
[32] F. M. Najafabadi, T. H. Rostami, K. Hosseinzadeh, D. D. Ganji. Thermal analysis of a moving fin using the radial basis function approximation" Heat transfer, 50(8)(2021): 7553-7567.
[33] M. G. Sobamowo , A. A. Yinusa, O. P. Popoola, M. A. Waheed. Transient Thermal Analysis of Convective-Radiative Moving Fin under the Influences of Magnetic Field and Time-dependent Boundary Condition. Computational Sciences and Engineering 1(2) (2021) 139-152.
[34] J. Ma, Y. Sun, B. Li. Spectral collocation method for transient thermal analysis of coupled conductive, convective and radiative heat transfer in the moving plate with temperature dependent properties and heat generation. International Journal of Heat and Mass Transfer 114 (2017) 469–482.
[35] J. Ma, Y. Sun, B. Li. Simulation of combined conductive, convective and radiative heat transfer in moving irregular porous fins by spectral element method. International Journal of Thermal Sciences 118 (2017) 475-487.
[36] S. Hosseinzadeh, K. Hosseinzadeh, A. Hasibi, D.D. Ganji, Thermal analysis of moving porous fin wetted by hybrid nanofluid with trapezoidal, concave parabolic and convex cross sections, *Case Studies in Thermal Engineering* (2022), doi: https://doi.org/10.1016/j.csite.2022.101757.

[37] M. Turkyilmazoglu. Stretching/shrinking longitudinal fins of rectangular profile and heat transfer. Energy Conversion and Management 91 (2015) 199–203.
[38] M., Turkyilmazoglu. Expanding/contracting fin of rectangular profile. International journal of numerical methods for heat & fluid flow, 31(4)(2021), 1057-1068.
[39] D. Bhanja, B. Kundu, A. Aziz . Enhancement of heat transfer from a continuously moving porous fin exposed in convective–radiative environment. Energy Conversion and Management 88 (2014) 842-853.
[40] Y. S. Sun and J. L. Xu. Thermal performance of continuously moving radiative–convective fin of complex cross-section with multiple nonlinearities. International Communications in Heat and Mass Transfer 63 (2015) 23–34.
[41] P. K. Roy, A. Mallick, H. Mondal and P. Sibanda. A modified decomposition solution of triangular moving fin with multiple variable thermal properties. Arabian Journal for Science and Engineering. 43(3)(2018), 1485-1497.
[42] G. Sowmya, I. E. Sarris, C. S. Vishalakshi, R. S.V. Kumar, B. C. Prasannakumara. Analysis of Transient Thermal Distribution in a Convective–Radiative Moving Rod Using Two-Dimensional Differential Transform Method with Multivariate Pade Approximant. Symmetry 2021, 13, 1793.
[43] H. Chen, J. Ma, H. Liu. Least square spectral collocation method for nonlinear heat transfer in moving porous plate with convective and radiative boundary conditions. International Journal of Thermal Sciences 132 (2018) 335–343
[44] S. Saedodin, M. Sadegh M. Barforoush. Comprehensive analytical study for convective–radiative continuously moving plates with multiple non-linearities. Energy Conversion and Management 81 (2014) 160–168.
[45] S. Ullah, A. Alli, Z. U. Din. Heat transfer analysis in stretching/shrinking rectangular fin with convection and radiation. Mathematical Methods in the Applied Sciences. Article in Press
[46] B. J. Gireesha, G. Sowmya, M. Nikitha. Numerical Investigation of Natural Convection and Radiation In a Moving Radial Porous Fin Journal of Engineering & Management, Volume 4, No.1, January – June 2020
[47] M. G. Sobamowo. Finite element thermal analysis of a moving porous fin with temperature-variant thermal conductivity and internal heat generation Reports in Mechanical Engineering 1(1)(2020), 110-127.
[48] S. Singh, D. Kumar and K. N. Rai. Convective-radiative fin with temperature-dependent thermal conductivityy, heat transfer coefficient and wavelength-dependent surface emissivity. Propulsion and Power Research. 3(4)(2014), 207–221.
[49] M. G. Sobamowo, M. O. Salami, A. A. Yinusa. Thermal Analysis of a Convective-Radiative Moving Porous Trapezoidal Fin with Variable Thermal Properties and Internal Heat Generation using Finite Element Method. World Scientific News 163 (2022) 139-157.
[50] M. Nabati, · S. Taherifar · M. Jalalvand. Sinc–Galerkin approach for thermal analysis of moving porous fin subject to nanoliquid flow with different shaped nanoparticles. Mathematical Sciences
[51] B. J. Gireesha, G Sowmya and Rama Subba Reddy Gorla. Nanoparticle shape effect on the thermal behaviour of moving longitudinal porous fin. Proc IMechE Part N: J Nanomaterials, Nanoengineering and
Nanosystems, 1–7.
[52] B. J. Gireesha, G. Sowmya, M. I. Khan, *et al.* Flow of hybrid nanofluid across a permeable longitudinal moving fin along with thermal radiation and natural convection. Comput Meth Prog Bio 2019; 185: 105166.
[53] M. Turkyilmazoglu. Efficiency of the longitudinal fins of trapezoidal profile in motion. Journal of Heat Transfer. 2017. 30(4)(2020), 1867-1879
[54] M. G. Sobamowo and M. A. Waheed. Analytical investigation of heat transfer in a moving convective porous fin with temperature dependent thermal conductivity and internal heat generation. World Scientific News 150 (2022) 1-21.

[55] P. L. Ndlovu and R. J. Moitsheki. Steady state heat transfer analysis in a rectangular moving porous fin. Propulsion and Power Research 2020
[56] G. A. Oguntala, M. G. Sobamowo, A. A. Yinusa and R. ABD-Alhameed. Determination of Proper Fin Length of a Convective-Radiative Moving Fin of Functionally Graded Material Subjected to Lorentz Force. Defect and Diffusion Forum, 401, 14-24
[57] B.J. Gireesha , G. Sowmya , M. I. Khan , H. F. Oztop , Flow of hybrid nanofluid across a permeable longitudinal moving fin along with thermal radiation and natural convection, Computer Methods and Programs in Biomedicine (2019).
[58] M. G. Sobamowo, O. M. Kamiyo, A. A. Yinusa, and M. O. Salami. Exploration of the effects of fin geometry and material properties on thermal performance of convective-radiative moving fins. Eng. Appl. Sci. Lett. 2019, 2(3), 14-29
[59] M. G. Sobamowo, O. M. Kamiyo, M. O. Salami, A. A. Yinusa. Thermal assessment of a convective porous moving fins of different material properties using Laplace-variational iterative method. World Scientific News 139(2) (2020) 135-154.
[60] Y. Jaluria, A.P. Singh, Temperature distribution in a moving material subjected to surface energy transfer, Computer Methods in Applied Mechanics and Engineering 41 (1983) 145–156.
[61] Y. Jaluria. Transport from continuously moving materials undergoing thermal processing, Annual Reviews of Heat Transfer, vol. 4, Academic Press, 1992, pp. 187–245 (Chapter Four).
[62] C.-H. Chen, Convection cooling of a continuously moving in manufacturing processes, Journal of Materials Processing Technology 138 (2003) 332–338.
[63] E.M. Sparrow, J.P. Abraham, Universal solutions for the streamwise variation of the temperature of a moving sheet in the presence of a moving fluid, International Journal of Heat and Mass Transfer 48 (2005) 3047–3056.
[64] M.V. Karwe, Y. Jaluria, Thermal transport from a heated moving surface, ASME Journal of Heat Transfer 108 (1986) 728–733.
[65] M.V. Karwe, Y. Jaluria, Fluid flow and mixed convection transport from a plate in rolling and extrusion processes, ASME Journal of Heat Transfer 110 (1988) 635–661.
[66] M.V. Karwe, Y. Jaluria, Numerical simulation of thermal transport associated with a continuously moving flat sheet in materials processing, ASME Journal of Heat Transfer 113 (1991) 612–619.
[67] R. M. Simon, M. T Stroot, G. H Weiss. Numerical inversion of Laplace transforms with application to percentage labeled mitoses experiments. Computers and Biomedical Research. 5 (1972), 596-607.
[68] H. A. Hoshyar, I. Rahimipetroudi, D. D. Ganji, & A. R. Majidian (2015). Thermal performance of porous fins with temperature-dependent heat generation via the homotopy perturbation method and collocation method. *Journal of Applied Mathematics and Computational Mechanics*, 14(4), 53-65.
[69] O. Güngör, C. Arslantürk. Thermal analysis of longitudinal a porous fin with temperature-dependent internal heat generation using the variation of parameters method. *Journal of Applied Mathematics and Computational Mechanics* 2020, 19(3), 5-16